IYBSSD2022
International Year
of Basic Sciences
for Sustainable Development

Updated constraints on sterile neutrino mixing in the OPERA experiment using a new ν_e identification method

OPERA Collaboration, N. Agafonova[1], A. Alexandrov[2], A. Anokhina[3], S. Aoki[4],
A. Ariga[5], T. Ariga[5,6], A. Bertolin[7], C. Bozza[8], R. Brugnera[7,9], S. Buontempo[2],
M. Chernyavskiy[10], A. Chukanov[11], L. Consiglio[2], N. D'Ambrosio[12],
G. De Lellis[2,13,14], M. De Serio[15,16], P. del Amo Sanchez[17], A. Di Crescenzo[2,13],
D. Di Ferdinando[18], N. Di Marco[12], S. Dmitrievsky[11], M. Dracos[19],
D. Duchesneau[17], S. Dusini[7], T. Dzhatdoev[3], J. Ebert[20], A. Ereditato[5], R. A. Fini[16],
T. Fukuda[21], G. Galati[2,13,38], A. Garfagnini[7,9], V. Gentile[22], J. Goldberg[23],
S. Gorbunov[10], Y. Gornushkin[11], G. Grella[8], A. M. Guler[24], C. Gustavino[25],
C. Hagner[20], T. Hara[4], T. Hayakawa[21,★], A. Hollnagel[20], K. Ishiguro[21], A. Iuliano[2,13],
K. Jakovčć[26], C. Jollet[19], C. Kamiscioglu[24,27], M. Kamiscioglu[24], S. H. Kim[28],
N. Kitagawa[21], B. Kliček[29], K. Kodama[30], M. Komatsu[21], U. Kose[7,39], I. Kreslo[5],
F. Laudisio[7,9], A. Lauria[2,13], A. Longhin[7,9], P. Loverre[25], A. Malgin[1], G. Mandrioli[18],
T. Matsuo[31], V. Matveev[1], N. Mauri[18,32], E. Medinaceli[7,40], A. Meregaglia[19],
S. Mikado[33], M. Miyanishi[21], F. Mizutani[4], P. Monacelli[25], M. C. Montesi[2,13],
K. Morishima[21], M. T. Muciaccia[15,16], N. Naganawa[21], T. Naka[31], M. Nakamura[21],
T. Nakano[21], K. Niwa[21], S. Ogawa[31], N. Okateva[10], K. Ozaki[4], A. Paoloni[34],
L. Paparella[15,16], B. D. Park[28,41], L. Pasqualini[18,32], A. Pastore[16], L. Patrizii[18],
H. Pessard[17], D. Podgrudkov[3], N. Polukhina[10,35], M. Pozzato[18], F. Pupilli[7],
M. Roda[7,9,42], T. Roganova[3], H. Rokujo[21], G. Rosa[25], O. Ryazhskaya[1], O. Sato[21],
A. Schembri[12], I. Shakiryanova[1], T. Shchedrina[10], E. Shibayama[4], H. Shibuya[31,43],
T. Shiraishi[21], S. Simone[15,16], C. Sirignano[7,9], G. Sirri[18], A. Sotnikov[11], M. Spinetti[34],
L. Stanco[7], N. Starkov[10], S. M. Stellacci[8], M. Stipčevic[29], P. Strolin[2,13], S. Takahashi[4],
M. Tenti[18], F. Terranova[36], V. Tioukov[2], S. Tufanli[5,44], S. Vasina[11], P. Vilain[37,†],
E. Voevodina[2], L. Votano[34], J. L. Vuilleumier[5], G. Wilquet[37], and C. S. Yoon[28]

[1]*INR – Institute for Nuclear Research of the Russian Academy of Sciences, RUS-117312 Moscow, Russia*
[2]*INFN Sezione di Napoli, I-80126 Napoli, Italy*
[3]*SINP MSU – Skobeltsyn Institute of Nuclear Physics, Lomonosov Moscow State University, RUS-119991 Moscow, Russia*
[4]*Kobe University, J-657-8501 Kobe, Japan*
[5]*Albert Einstein Center for Fundamental Physics, Laboratory for High Energy Physics (LHEP), University of Bern, CH-3012 Bern, Switzerland*
[6]*Faculty of Arts and Science, Kyushu University, J-819-0395 Fukuoka, Japan*
[7]*INFN Sezione di Padova, I-35131 Padova, Italy*
[8]*Dipartimento di Fisica dell'Università di Salerno and "Gruppo Collegato" INFN, I-84084 Fisciano (Salerno), Italy*
[9]*Dipartimento di Fisica e Astronomia dell'Università di Padova, I-35131 Padova, Italy*
[10]*LPI – Lebedev Physical Institute of the Russian Academy of Sciences, RUS-119991 Moscow, Russia*

[11] *JINR – Joint Institute for Nuclear Research, RUS-141980 Dubna, Russia*

[12] *INFN – Laboratori Nazionali del Gran Sasso, I-67010 Assergi (L'Aquila), Italy*

[13] *Dipartimento di Fisica dell'Università Federico II di Napoli, I-80126 Napoli, Italy*

[14] *CERN, European Organization for Nuclear Research, CH-1211, Geneva, Switzerland*

[15] *Dipartimento di Fisica dell'Università di Bari, I-70126 Bari, Italy*

[16] *INFN Sezione di Bari, I-70126 Bari, Italy*

[17] *LAPP, Université Savoie Mont Blanc, CNRS/IN2P3, F-74941 Annecy-le-Vieux, France*

[18] *INFN Sezione di Bologna, I-40127 Bologna, Italy*

[19] *IPHC, Université de Strasbourg, CNRS/IN2P3, F-67037 Strasbourg, France*

[20] *Hamburg University, D-22761 Hamburg, Germany*

[21] *Nagoya University, J-464-8602 Nagoya, Japan*

[22] *GSSI – Gran Sasso Science Institute, I-40127 L'Aquila, Italy*

[23] *Department of Physics, Technion, IL-32000 Haifa, Israel*

[24] *METU – Middle East Technical University, TR-06800 Ankara, Turkey*

[25] *INFN Sezione di Roma, I-00185 Roma, Italy*

[26] *Rudj er Bošković Institute, HR-10000 Zagreb, Croatia*

[27] *Ankara University, TR-06560 Ankara, Turkey*

[28] *Gyeongsang National University, 501 Jinju-daero, Jinju, Korea*

[29] *Center of Excellence for Advanced Materials and Sensing Devices, Ruder Bošković Institute, HR-10000 Zagreb, Croatia*

[30] *Aichi University of Education, J-448-8542 Kariya (Aichi-Ken), Japan*

[31] *Toho University, J-274-8510 Funabashi, Japan*

[32] *Dipartimento di Fisica e Astronomia dell'Università di Bologna, I-40127 Bologna, Italy*

[33] *Nihon University, J-275-8576 Narashino, Chiba, Japan*

[34] *INFN – Laboratori Nazionali di Frascati dell'INFN, I-00044 Frascati (Roma), Italy*

[35] *MEPhI – Moscow Engineering Physics Institute, RUS-115409 Moscow, Russia*

[36] *Dipartimento di Fisica dell'Università di Milano-Bicocca, I-20126 Milano, Italy*

[37] *IIHE, Université Libre de Bruxelles, B-1050 Brussels, Belgium*

[38] *Present address: University of Bari Aldo Moro*

[39] *Present address: CERN*

[40] *Present address: INAF–OAS Bologna, Italy*

[41] *Present address: Samsung Changwon Hospital, SKKU, Changwon, Korea*

[42] *Present address: University of Liverpool, Liverpool, UK*

[43] *Present address: Kanagawa University, J-221-8686 Yokohama, Japan*

[44] *Present address: Yale University, New Haven, CT 06520, USA*

[*]E-mail: hayakawa@flab.phys.nagoya-u.ac.jp

[†]Deceased.

To the memory of Prof. Pierre Vilain.

. . . .

This paper describes a new ν_e identification method specifically designed to improve the low-energy ($< 30\,\text{GeV}$) ν_e identification efficiency attained by enlarging the emulsion film scanning volume with the next-generation emulsion readout system. A relative increase of 25–70% in the ν_e low-energy region is expected, leading to improvements in the OPERA sensitivity to neutrino oscillations in the framework of the $3 + 1$ model. The method is applied to a subset of data where the detection efficiency increase is expected to be more relevant, and one additional ν_e candidate is found. The analysis combined with the ν_τ appearance results improves the upper limit on $\sin^2 2\theta_{\mu e}$ to 0.016 at 90% C.L. in the Mini-BooNE allowed region $\Delta m_{41}^2 \sim 0.3\,\text{eV}^2$.

. . . .

Subject Index   C04, C32

1.   Introduction

Oscillations among three neutrino flavors have been established by solar, atmospheric, reactor, and long-baseline accelerator neutrino experiments [1–7] over the last two decades. On the other hand, the presence of additional sterile neutrinos could explain the excess of ν_e and $\overline{\nu}_e$ charged-current events in short-baseline accelerator experiments—LSND [8] and MiniBooNE [9,10]—and the deficits of ν_e and $\overline{\nu}_e$ from radioactive-source and reactor experiments [11–13].

The OPERA experiment was operated as a long-baseline neutrino oscillation experiment performed to observe the appearance of ν_τ in a ν_μ beam through the identification of their charged-current (CC) interactions in a lead-plate target instrumented with high-resolution nuclear emulsion films [14]. The OPERA detector was exposed to the CERN Neutrinos to Gran Sasso (CNGS) ν_μ beam [15] with a mean energy of about 17 GeV and was located at the LNGS underground laboratory, 732 km away from the neutrino source. As a result of the data taking and the analysis, the OPERA Collaboration reported the discovery of a ν_τ appearance with a significance of 6.1σ [16,17] and the results of a search for ν_e CC interactions in excess of expectation from the beam contamination [18]. In the combined analysis of these two appearance modes [19], the 90% C.L. upper limit on $\sin^2 2\theta_{\mu e} = 4|U_{\mu 4}|^2|U_{e4}|^2$ was set to 0.019 for $\Delta m_{41}^2 > 0.1\,\mathrm{eV}^2$, and the MiniBooNE best-fitting values, $\Delta m_{41}^2 = 0.043\,\mathrm{eV}^2$, $\sin^2 2\theta = 0.807$ [10], were excluded.

Since the ν_μ beam flux drops above 30 GeV, a high ν_e detection efficiency for the low-energy (< 30 GeV) region is crucial for the ν_e appearance search. However, the ν_e detection method used in the previous analysis [18] has efficiencies of 10–40% for this energy region, because of the limited analysis capability due to the speed of emulsion readout systems at that time [20,21]. Today, a 70 times faster scanning system makes it possible to improve the analysis [22]. In this paper we take advantage of this next-generation system to present a new ν_e identification method, report its performances, and update the constraint on the parameters of the $3 + 1$ neutrino mixing model.

2.   Detector, beam, and data sample

The OPERA detector was a hybrid apparatus made of nuclear emulsion trackers and electronic detectors [14]. The target was based on the emulsion cloud chamber (ECC) technology, consisting of alternating 57 emulsion films and 56 1 mm thick lead plates with a section of $12.7 \times 10.2\,\mathrm{cm}^2$. The total thickness of 7.5 cm was equivalent to about 10 radiation lengths. A pair of two films, called a changeable sheet (CS) [14], was attached externally on the downstream face of each ECC brick. The full detector had two identical super-modules (SM), each of which was segmented into a target section and a muon spectrometer. In the target sections, ECC bricks were arranged in 29 layers of walls interleaved with target trackers (TT), which were planes of horizontal and vertical scintillator strips. A spectrometer, consisting of two iron core magnets instrumented with resistive plate chambers (RPCs) and drift tubes, was mounted downstream of each instrumented target. It was aimed at identifying muons and measuring their charge sign and momentum. The two SMs contained about 150 000 ECC bricks corresponding to a total mass of 1.25 kt.

The CNGS beam was an almost pure ν_μ beam with a contamination of 2.0% $\overline{\nu}_\mu$, 0.8% ν_e, and 0.05% $\overline{\nu}_e$ [23] in terms of CC interactions. The mean energy was 17.9 GeV (ν_μ), 21.8 GeV ($\overline{\nu}_\mu$), 24.5 GeV (ν_e), and 24.4 GeV ($\overline{\nu}_e$). The prompt ν_τ contamination was negligible $\mathcal{O}(10^{-7})$.

During the CNGS beam exposure of 17.97×10^{19} protons on target, OPERA collected 19 505 on-time events in the fiducial volume. The ECC brick where a neutrino interaction has occurred was identified exploiting the pattern of the TT hits on-time with the CNGS beam. The track candidates in the CS are extrapolated to the ECC brick and searched upstream film by film. After location of the interaction vertex, $1 \times 1\,\text{cm}^2$ in 10 films downstream and five films upstream of the vertex were scanned and the tracks originating from the vertex were reconstructed. Finally, 5868 neutrino interactions were successfully reconstructed.

3. New ν_e identification method

The events with one reconstructed muon or with a total number of fired TT and RPC planes larger than 19 were tagged as 1μ and excluded from the analysis [16]. The remaining 1185 0μ events were targeted for the ν_e search.

The thickness of an ECC brick is enough to develop the electromagnetic (e.m.) showers produced by electrons originating from the ν_e CC interactions, whereas the scanning volume of $1\,\text{cm}^2$ and 10 films is equivalent to about 1.8 X_0. This scanning volume was limited by the scanning speed of the conventional readout systems [20,21]. Therefore, in the previous search, identification of ν_e CC interactions was performed by a method using CS tracks, called CS shower hint (CSH). A search is performed in the CS for track segments less than 2 mm apart from the extrapolation point of each track originating from the interaction vertex (primary tracks). Moreover, the direction of candidate CS tracks is required to be compatible within 150 mrad with that of the primary track. If at least three such tracks are found, additional scanning along the primary track is performed aiming at the detection of an e.m. shower [24]. However, the identification efficiency of ν_e CC events using the CSH method decreases with ν_e energy because the probability for the e.m. shower to be absorbed in the ECC brick and not be able to reach the CS increases, especially if the interaction takes place in the most upstream part of the ECC brick. Improving the efficiency of detecting low-energy e.m. showers inside the ECC brick would increase the identification efficiency for low-energy ν_e. To achieve this, a next-generation emulsion readout system (hyper-track selector, HTS) [22] with a scanning speed 70 times faster than conventional ones, has been introduced to enable enlargement of the scanning volume.

The new ν_e identification method in ECC, hereafter called ECC shower detection (ESD), is defined as shown in Fig. 1. A volume of $5 \times 5\,\text{cm}^2$ and 20 films downstream from the vertex are scanned by HTS. After track reconstruction, the cones from the vertex with an apex angle of 0.06 rad containing at least 10 track segments pointing to the vertex within a tolerance of 0.1 rad are tagged as e.m. shower candidates. These parameters have been optimized to keep a high detection efficiency while reducing noise. Tracks without showers and e^+e^- pairs arising from at least two films downstream of the vertex are removed from the shower candidates by a visual scan, while the other background sources are also removed by the selection described below. The remaining candidates are identified as ν_e.

The ν_e identification efficiency has been evaluated by a detailed Monte Carlo (MC) simulation with the standard OPERA simulation framework [25], based on the CNGS beam fluxes estimated by FLUKA [26,27] and the neutrino interactions generated by GENIE v2.8.6 [28,29]. Here we describe the expected ν_e identification efficiency and number of ν_e CC interactions when analyzing the full data set, i.e., all 0μ events located in the ECC bricks. The detection

(a) Scanning volume and shower detection cone.   (b) Track segment selection criteria.
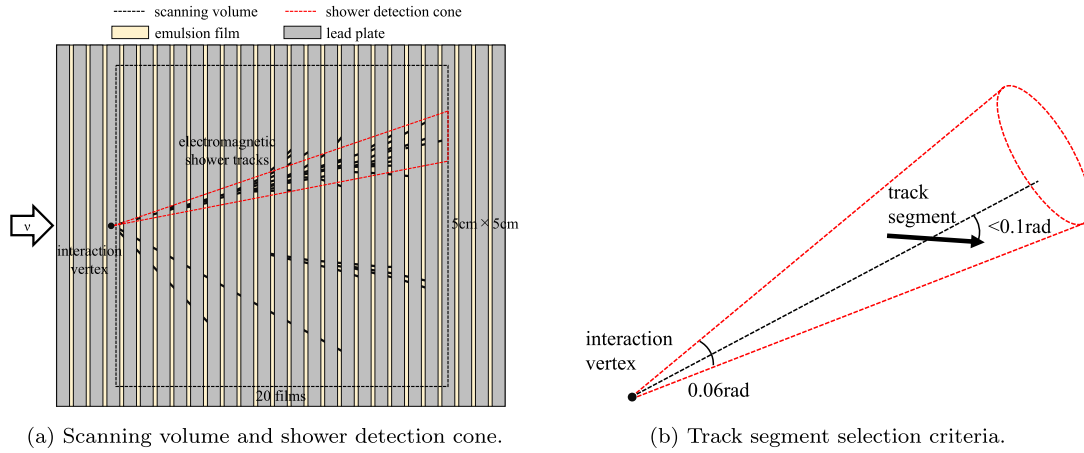
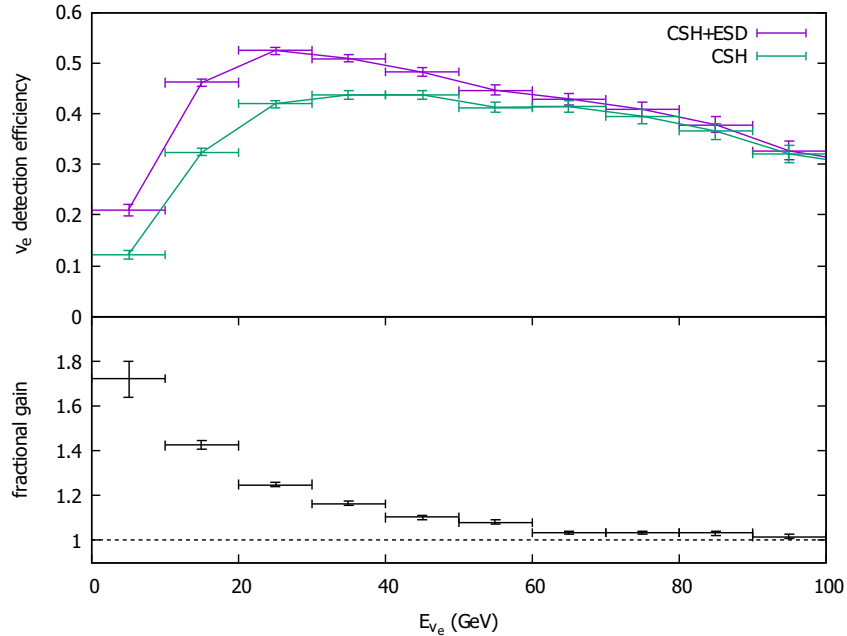**Fig. 1.** The concept of the ECC shower detection (ESD) method.

Fig. 2. The top plot shows the ν_e detection efficiency and its statistical uncertainty as a function of the ν_e energy. The bottom plot shows the fractional gain of the efficiency, i.e., the ratio of the ESD+CSH efficiency and the CSH efficiency.

efficiency of track segments, the position and angle accuracy, the track reconstruction, and the shower detection process mentioned above with HTS are taken into account. The estimated ν_e identification efficiency is shown in Fig. 2; the improvement by adding the ESD method is about 25–70% below 30 GeV. The expected number of ν_e CC candidates of the full data set without any other background in the no-oscillation hypothesis increases from 31.0 ± 0.9 (stat.) ± 3.0 (syst.) when using the CSH method only to 36.7 ± 1.1 (stat.) ± 3.2 (syst.) when both the CSH and ESD methods are used. The improvement of the sensitivity for $\sin^2 2\theta_{\mu e}$ in the MiniBooNE allowed region $\Delta m^2_{41} \sim 0.3$ is expected to be 28% by applying an energy spectrum analysis with the improved efficiency in the low-energy region where it is more sensitive to the oscillations.

The ESD method has higher detection efficiency for low-energy e.m. showers than the previous one; consequently it increases the backgrounds for the ν_e CC interaction search. The background sources are classified as follows: (1) e^+e^- pairs produced by prompt conversion of γ-rays from π^0 decays, (2) random coincidence of single hadron tracks and e.m. shower tracks, (3) $\tau \to e$ decays from ν_τ CC interactions.

To limit/suppress the prompt γ conversion background (1), a single electron track is searched for at the most upstream film in the scanning volume. The single electron classification requires that, in the region within $70\,\mu$m and 0.3 rad from the primary electron candidate at the most upstream film, only hadron tracks are found or at most an even number of electron-like tracks. All tracks consisting of eight or more track segments and no e.m. showers are classified as hadrons. An e^+e^- pair is misidentified as a single electron when one of the pair electrons is scattered out of the specified range for this criteria. In addition, the energy of the e.m. shower, estimated by a neural-network-based method using shower properties [30], is to be at least 1.1 GeV. These conditions have been determined to maximize the statistical significance of the ν_e appearance.

Random coincidences of hadron and shower tracks (2) occur in 10% of all 0μ events. They can be reduced by evaluating the probability that the primary electron candidate is a hadron. Thus a maximum likelihood estimation with the following four variables [30] is applied: (a) minimum opening angle between the primary electron candidate and all e^+e^- pair directions, (b) ratio of the momentum of the primary electron candidate measured in the 1st–9th plates relative to the 10th–18th plates from the most upstream film, (c) number of films that the primary electron candidate penetrates, (d) mean azimuthal opening angle between the primary electron candidate and the hadrons.

The conditions for $\tau \to e$ decays (3) to be identified as ν_τ CC interactions are given in Ref. [17]. Conversely, they are wrongly identified as ν_e when they do not satisfy these conditions. After such selection, the expected numbers of backgrounds (1), (2), and (3) with their systematic uncertainty together with CSH are 2.6 ± 0.9, 1.2 ± 0.5, and 1.5 ± 0.3, respectively.

4.　Analysis sample

In this section, we describe the result of the application of the ESD method to a subsample of 0μ events. In order to balance the requested additional scanning load and the expected number of additional ν_e candidates, we have selected a subsample according to the following criteria: the events have neutrino interactions in the upstream part of the ECC brick (film number < 18, which is 7–10 X_0 deep from the downstream side of the ECC brick) and are contained within the volume of ECC brick at least 5 mm away from the film edge, they show at least two reconstructed particles at the vertex, and have not been identified as ν_e candidates by the CSH method. These criteria selected a sample of 99 events. Figure 3 shows the ν_e identification efficiency as a function of the vertex film number (the number of the film immediately downstream of the vertex) for located events of energy $E_{\nu_e} < 30\,$GeV, indicating that the efficiency improvement is higher for ν_e CC interactions located in the upstream part of the ECC brick.

The result of the scanning and the analysis is summarized in Table 1. In the target events, 91 events were fully analyzed, while eight were discarded due to failures in the analysis procedure. Track reconstruction failure is caused by the bad quality of the films and does not introduce
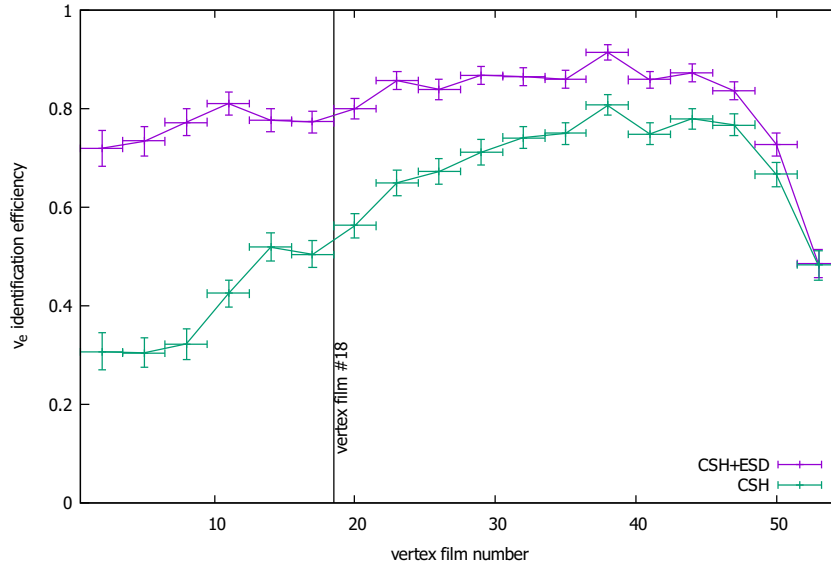
Fig. 3. The ν_e identification efficiency as a function of vertex film number, for located events of energy $E_{\nu_e} < 30$ GeV. The beam enters the ECC brick through film #1 and the CS is attached on the opposite side.

Table 1. Breakdown of the analysis result in terms of number of events.

Analysis completed	e.m. shower found	ν_e candidate	1
		γ conversion	47
	no e.m. showers		43
Discarded	track reconstruction failure		5
	vertex confirmation failure		3
Total			99

biases; thus corresponding cases should be removed in the normalization procedure described below. In contrast, the failure of vertex confirmation may produce a bias since it is likely associated with a lower track multiplicity at the primary vertex. However, the expected bias is estimated to be less than 1%, smaller than the systematic uncertainty.

Electromagnetic showers were found in the analyzed volume of 48 events, and one of them was identified as a ν_e CC interaction candidate with a reconstructed energy of (80 ± 36) GeV. A total of 14 events were observed in energy above 50 GeV, while the expected numbers of ν_e candidates from each source for this energy range are 0.04 ($\nu_\mu \to \nu_e$ ESD), 3.14 ($\nu_\mu \to \nu_e$ CSH), 0.11 ($\nu_e \to \nu_e$ ESD), 9.16 ($\nu_e \to \nu_e$ CSH), and 0.15 (other backgrounds) on the assumption of the $3 + 1$ mixing model with the same parameters as used in Fig. 4(b). The total number of observed ν_e candidates, including those detected by the CSH method, is 36.

The expected number of prompt ν_e CC events in the absence of oscillation has been estimated using the CNGS flux, the neutrino cross section, and the detection efficiency evaluated by the MC simulation incorporating the above-mentioned subsample selection. The normalization for the CSH method is described in Ref. [18], and for the ESD method the same normalization as CSH is applied with the 91 fully analyzed events. The systematic uncertainty on the expected number of events results from the combination of different uncertainties, some of which are
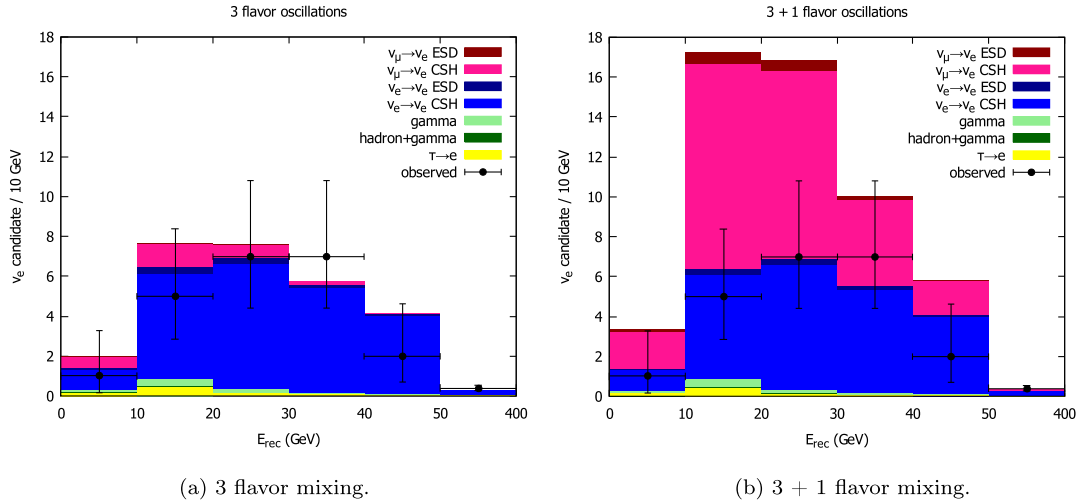
(a) 3 flavor mixing.   (b) $3 + 1$ flavor mixing.

Fig. 4. Reconstructed energy distribution of expected and observed ν_e candidates on the assumption of (a) 3-flavor mixing and (b) $3 + 1$-flavor mixing with $\Delta m^2_{41} = 0.269\,\mathrm{eV}^2$, $\sin^2 2\theta_{\mu e} = 0.019$, and $P(\nu_e(\bar{\nu}_e) \to \nu_e(\bar{\nu}_e)) \simeq 1$.

Table 2. Breakdown of the systematic uncertainties for the ν_e detection efficiencies of the CSH and ESD methods.

		$< 10\,\mathrm{GeV}$	$\geq 10\,\mathrm{GeV}$
Flux, cross section, and location		14%	6%
CSH identification		15%	8%
ESD identification	Track detection efficiency with HTS	15%	9%
	Difference of actual process with MC	4%	3%
	Statistical uncertainty in MC	20%	10%
	Overall in ESD identification	25%	14%
Overall		19%	10%

common to both the CSH and ESD methods (CNGS flux, neutrino cross section, and vertex location procedure), and the rest are specific (scanning and track reconstruction procedures including visual scan by a human and MC sample statistics) and weighted by the ratio of the selected samples and the detection efficiencies between the two methods. The breakdown of them is shown in Table 2. The contribution to the systematic error specific to the ESD method has been estimated to be 25%/14% for energies below/above 10 GeV, dominated by the limited size of the MC sample and the HTS track reconstruction efficiency. The overall systematic uncertainty is 19%/10% [30].

Other background sources such as prompt γ conversions, random coincidences between hadron and e.m. shower tracks, and $\tau \to e$ decays have been estimated by the same MC simulation, using the same normalization as for the ν_e CC events (Table 3). The combined systematic uncertainty of these background sources is dominated by the limited MC sample statistics and estimated to be 36% [30].

The expected numbers of ν_e candidates from the beam incorporating the subsample selection are summarized in Table 3. It should be noted that the total number of expected ν_e candidates by the ESD method with energy $< 30\,\mathrm{GeV}$ is 1.0 ± 0.2. The decreases in the expectations of the

Table 3. The expected number of ν_e candidates from each source under the assumption of no oscillations and with the CSH and ESD methods applied to the subsamples.

	beam ν_e	hadron $+\gamma$	γ	$\tau \to e$
CSH	31.0 ± 3.0	negligible	0.5 ± 0.5	0.7 ± 0.2
ESD	1.1 ± 0.1	0.1 ± 0.1	0.3 ± 0.2	0.05 ± 0.01

(a)   (b)
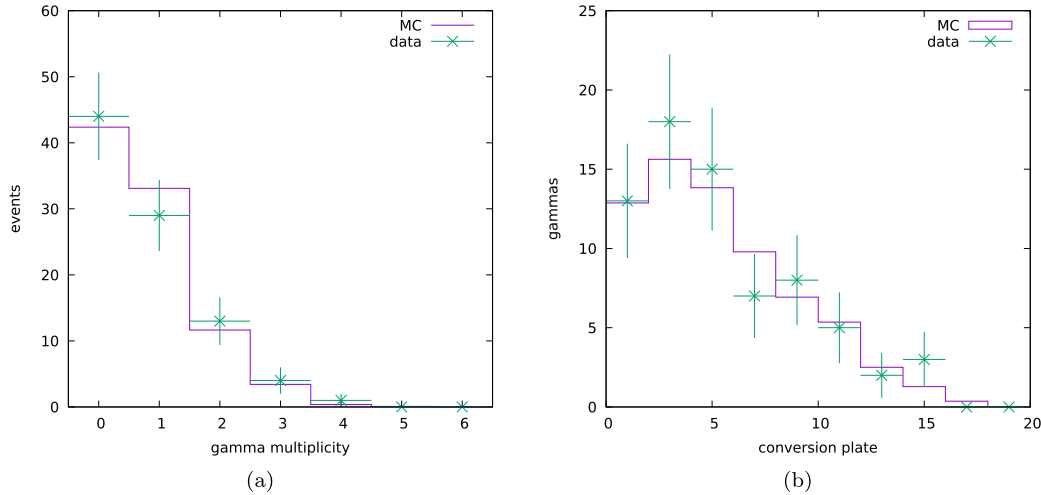
Fig. 5. γ-ray multiplicity (left) and conversion plate number from the vertex (right).

γ and hadron $+\gamma$ from the numbers with the full data set are greater than that of the beam ν_e. One of the major reasons for this is that the vertex film distributions of the γ-ray backgrounds are quite different from the beam ν_e because of the small e.m. shower energies, and another is that the γ-ray backgrounds have large statistical errors in the MC simulation.

The reconstructed energy distributions of expected and observed ν_e candidates are shown in Fig. 4. The oscillation parameters from Ref. [31] are used for the 3-flavor mixing model. For the $3 + 1$ mixing model, parameters on the intersection between the MiniBooNE allowed region [10] and the OPERA exclusion border [19], i.e., $\Delta m_{41}^2 = 0.269 \, \text{eV}^2$, $\sin^2 2\theta_{\mu e} = 0.019$, and $P(\nu_e(\overline{\nu}_e) \to \nu_e(\overline{\nu}_e)) \simeq 1$, are assumed. The total expected number of ν_e candidates from prompt ν_e, $\overline{\nu}_e$ and all other backgrounds is 34.0 ± 3.3.

As already mentioned, the ESD method has a high sensitivity for low-energy e.m. showers; therefore the comparison of the observed γ-ray properties to the expectation is useful for the validation of this method. In Fig. 5, the distribution of the γ-ray multiplicity—the number of γ-rays detected per event—and their free path before conversion obtained from the MC simulation are compared to those of the observed γ-rays. The number of events in the MC simulation is normalized with the number of fully analyzed events. Both MC distributions are well consistent with experimental data, and the expected number of γ-rays, 69 ± 11, is in agreement with the observed one, 71.

5. Oscillation analysis in the $3 + 1$ mixing model

In order to check the presence of a light sterile neutrino as suggested by the LSND and Mini-BooNE experimental results, the $3 + 1$-flavor mixing model is assumed. Not only ν_e but also ν_τ appearance searches were conducted by the OPERA Collaboration [17]. Since the ν_τ flux
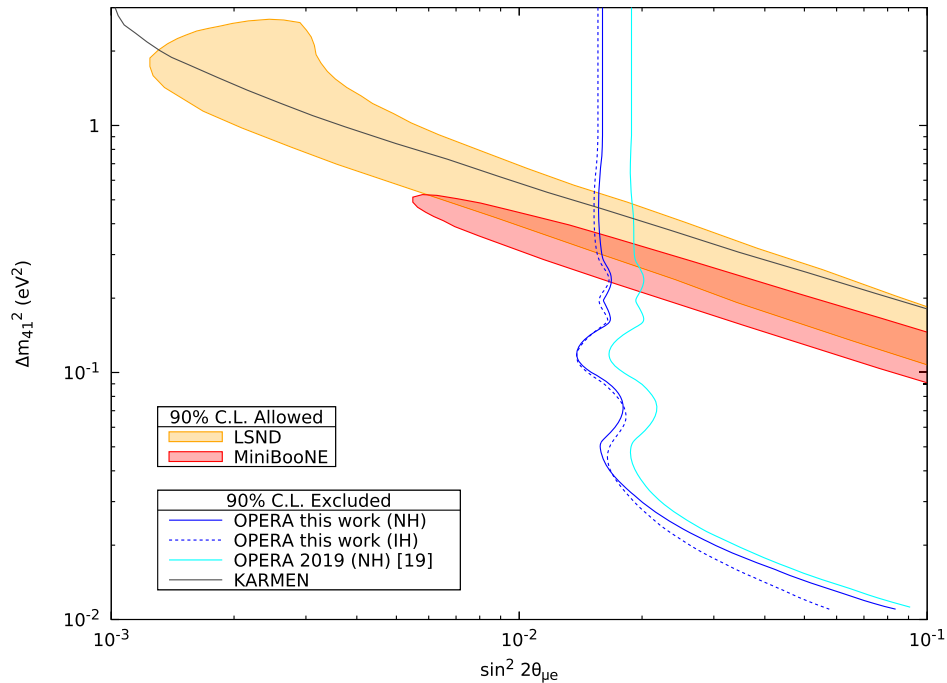
Fig. 6. The 90% C.L. exclusion region in the Δm_{41}^2 and $\sin^2 2\theta_{\mu e}$ plane for the normal (NH, solid) and inverted (IH, dashed) hierarchies. The allowed region at 90% C.L. by LSND [8] and MiniBooNE [10] and the excluded region by the previous OPERA analysis [19] and KARMEN [32] are also shown. The region drawn above is completely excluded by the combined result of MINOS, MINOS+, Daya Bay, and Bugey-3 [33], which conducted ν_μ and ν_e disappearance analyses.

with the parameters used in Fig. 4(b) is expected to vary from almost 0 to 10 times larger than the 3-flavor mixing, and some parameter space allowed by only ν_e appearance analysis can be excluded, both appearance channels have been jointly used. The statistical analysis is based on the profile likelihood ratio by comparing the observed energy spectrum to the expectation under the 3 + 1-flavor mixing model. Δm_{41}^2 and $\sin^2 2\theta_{\mu e}$ are the parameters of interest. The value of Δm_{21}^2 is fixed to the PDG value [31], while a Gaussian constraint on Δm_{31}^2 is assumed with mean and sigma also found in Ref. [31]. The dependences on the other parameters are removed by treating them as nuisance parameters. More details are described in Ref. [19].

As the result of this test statistic, the 90% C.L. exclusion region obtained by using both the CSH and ESD methods is shown in Fig. 6. The upper limit around the MiniBooNE allowed region $\Delta m_{41}^2 \sim 0.3\,\mathrm{eV}^2$ has been lowered to $\sin^2 2\theta_{\mu e} < 0.016$.

6. Conclusions

A new ν_e identification method, called ESD, was introduced to improve the detection efficiency for low-energy ν_e events that are crucial to investigate the MiniBooNE allowed region in the 3 + 1 mixing model. The shower detection method was optimized to detect electron-induced showers, and the ν_e identification efficiency increased by up to 70% below 30 GeV.

We applied the method to a subsample of 99 0μ events with a vertex in the most upstream part of the ECC brick. We have found one new ν_e candidate with a reconstructed neutrino energy of (80 ± 36) GeV. The expected additional number of ν_e candidates is 1.5 ± 0.2, in particular 1.0 ± 0.2 for energies below 30 GeV. It is worth noting that the observed γ-rays from π^0 decays are in agreement in number and properties with the expectation.

The 3 + 1-flavor mixing model has been tested and the 90% C.L. constraints have been improved to $\sin^2 2\theta_{\mu e} < 0.016$ around the MiniBooNE allowed region $\Delta m_{41}^2 \sim 0.3\,\text{eV}^2$.

References

[1] Q. R. Ahmad et al.[SNO Collaboration], Phys. Rev. Lett. **87**, 071301 (2001).
[2] Y. Fukuda et al.[Super-Kamiokande Collaboration], Phys. Rev. Lett. **81**, 1562 (1998).
[3] T. Araki et al. [KamLAND Collaboration], Phys. Rev. Lett. **94**, 081801 (2005).
[4] F. P. An et al. [Daya Bay Collaboration], Phys. Rev. Lett. **108**, 171803 (2012).
[5] P. Adamson et al.[MINOS Collaboration], Phys. Rev. Lett. **112**, 191801 (2014).
[6] K. Abe et al. [T2K Collaboration], Nature **580**, 339 (2020).
[7] M. A. Acero et al. [NOvA Collaboration], Phys. Rev. Lett. **123**, 151803 (2019).
[8] A. Aguilar et al. [LSND Collaboration], Phys. Rev. D **64**, 112007 (2001).
[9] A. A. Aguilar-Arevalo et al.[MiniBooNE Collaboration], Phys. Rev. Lett. **121**, 221801 (2018).
[10] A. A. Aguilar-Arevalo et al. [MiniBooNE Collaboration], Phys. Rev. D **103**, 052002 (2021).
[11] G. Mention, M. Fechner, Th. Lasserre, Th. A. Mueller, D. Lhuillier, M. Cribier, and A. Letourneau, Phys. Rev. D **83**, 073006 (2011).
[12] M. A. Acero, Carlo Giunti, and Marco Laveder, Phys. Rev. D **78**, 073009 (2008).
[13] V. V. Barinov et al., Phys. Rev. Lett. **128**, 232501 (2022).
[14] R. Acquafredda et al. [OPERA Collaboration], J. Instrum. **4**, P04018 (2009).
[15] G. Acquistapace et al., CERN-98-02, INFN/AE-98/05. CNGS webpage, http://proj-cngs.web.cern.ch/proj-cngs.
[16] N. Agafonova et al. [OPERA Collaboration], Phys. Rev. Lett. **115**, 121802 (2015).
[17] N. Agafonova et al. [OPERA Collaboration], Phys. Rev. Lett. **120**, 211801 (2018).
[18] N. Agafonova et al. [OPERA Collaboration], J. High Energy Phys. **1806**, 151 (2018).
[19] N. Agafonova et al. [OPERA Collaboration], Phys. Rev. D **100**, 051301(R) (2019).
[20] K. Morishima and T. Nakano, J. Instrum. **5**, P04011 (2010).
[21] L. Arrabito et al., Nucl. Instrum. Meth. A **568**, 578 (2006).
[22] M. Yoshimoto, T. Nakano, R. Komatani, and H. Kawahara, Prog. Theor. Exp. Phys. **2017**, 103H01 (2017).
[23] G. Acquistapace et al., CERN Reports No. CERN-98-02 and No. INFN/AE-98/05.
[24] N. Agafonova et al. [OPERA Collaboration], J. High Energy Phys. **1307**, 004 (2013).
[25] N. Agafonova et al. [OPERA Collaboration], J. High Energy Phys **1311**, 036, (2013).
[26] T. T. Bohlen, F. Cerutti, M.P.W. Chin, A. Fasso, A. Ferrari, P.G. Ortega, A. Mairani, P.R. Sala, G. Smirnov, and V. Vlachoudis, Nucl. Data Sheets **120**, 211 (2014).
[27] A. Ferrari, P. R. Sala, A. Fasso, and J. Ranft, CERN-2005-010 (2005).
[28] C. Andreopoulos et al., Nucl. Instrum. Meth. A **614**, 87 (2010).

[29] C. Andreopoulos, C. Barry, S. Dytman, H. Gallagher, T. Golan, R. Hatcher, G. Perdue, and J. Yarba, arXiv:1510.05494 [hep-ph][Search inSPIRE].
[30] T. Hayakawa, CERN-OPEN-2022-016.
[31] P.A. Zyla et al. [Particle Data Group], Prog. Theor. Exp. Phys. **2020**, 083C01 (2020).
[32] B. Armbruster et al. [KARMEN Collaboration], Phys. Rev. D **65**, 112001 (2002).
[33] P. Adamson et al. [Daya Bay and MINOS+ Collaborations], Phys. Rev. Lett. **125**, 071801 (2020).